

Lattice calculation of the Collins-Soper kernel from the soft function

Anthony Francis¹, C.-J. David Lin^{1,2}, Wayne Morris¹, Yong Zhao³

¹Institute of Physics, National Yang Ming Chiao Tung University, Hsinchu 30010, Taiwan

²Centre for High Energy Physics, Chung-Yuan Christian University, Taoyuan 32023, Taiwan

³Physics Division, Argonne National Laboratory, Lemont, IL 60439, USA

Introduction

Central to our understanding of TMDs are the TMD soft function, S_q , and Collins-Soper (CS) kernel, γ_q , [1], [2]. The former appears in the factorization of TMD observables, while the latter governs the rapidity-evolution of TMDs:

$$\gamma_q(b_\perp, \mu) = \frac{d}{d\sqrt{\zeta}} \ln f^{\text{TMD}}(x, b_\perp, \mu, \zeta). \quad (1)$$

Since the CS kernel also governs the rapidity evolution of the soft function,

$$\gamma_q(b_\perp, \mu) = \frac{d \ln S(b_\perp, \varepsilon, y)}{dy} - \text{UV counterterms}, \quad (2)$$

these two objects are closely related, allowing one to obtain the CS kernel from a computation of the soft function.

Soft function from Euclidean complex-directional Wilson loops

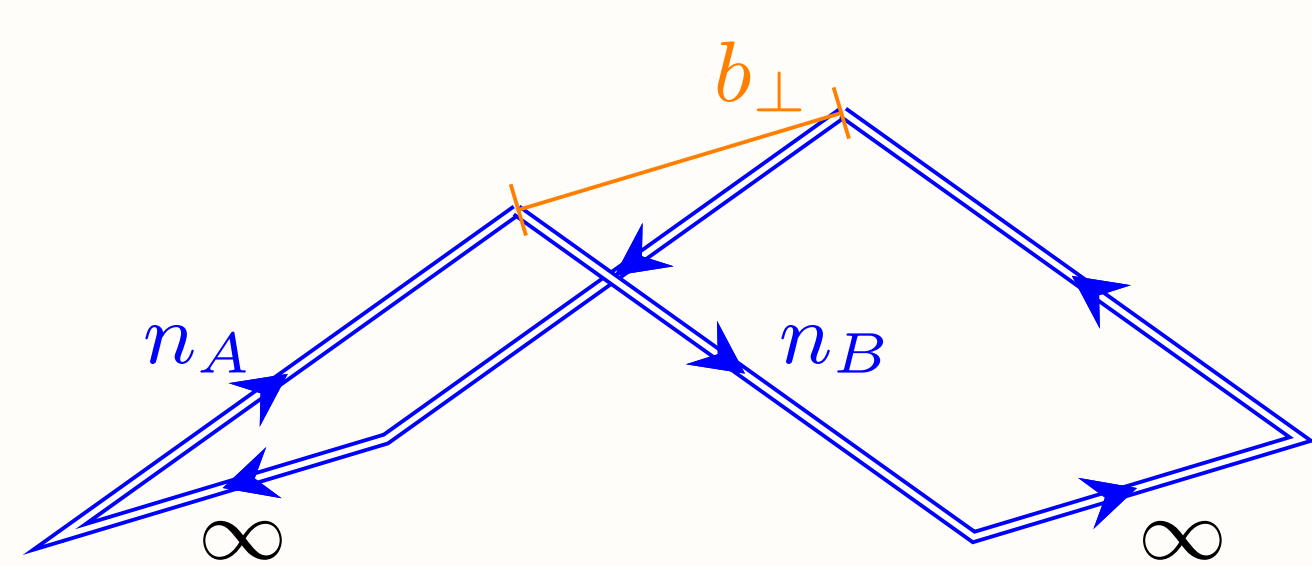


Figure 1: Schematic for soft function. The schematic for W_{bfly} will look the same, but with $\infty \rightarrow \tau$, and $y_{A/B} \rightarrow r_{a/b}$.

Minkowski space

- The soft factor, Fig. (1) suffers from rapidity divergences on the light-cone
- Directional vectors, n_A and n_B , regulate rapidity divergences [3]:

$$\begin{aligned} n_A &= \left(1 - e^{-2y_A}, \vec{0}_\perp, 1 + e^{-2y_A}\right), \\ n_B &= \left(1 - e^{-2y_B}, \vec{0}_\perp, -1 - e^{-2y_B}\right) \end{aligned} \quad (3)$$

- The soft factor at large rapidity is:

$$S_q(b_\perp, \mu, y_A - y_B) = S_I(b_\perp, \mu) e^{\gamma_q(b_\perp, \mu)(y_A - y_B)} + \mathcal{O}\left(e^{-2(y_A - y_B)}\right) \quad (4)$$

Euclidean space

- The analog to Eq. (3) in Euclidean space is:

$$\tilde{n}_A = (in_A^0, \vec{0}_\perp, n_A^3), \quad \tilde{n}_B = (in_B^0, \vec{0}_\perp, -n_B^3) \quad (5)$$

- Confirmed via one-loop computation, we have:

$$r_a = \frac{n_A^3}{n_A^0} = \frac{1 + e^{-2y_A}}{1 - e^{-2y_A}}, \quad r_b = \frac{n_B^3}{n_B^0} = \frac{1 + e^{2y_B}}{1 - e^{2y_B}}, \quad (6)$$

$$|r_a|, |r_b| > 1, \quad n_A^0 n_B^0 (r_a r_b + 1) > 0$$

- For finite length, L , Wilson lines we encounter power divergences, b_\perp/a , where a is the lattice spacing

Auxiliary propagator

- We can model the Wilson line as a one-dimensional auxiliary field [4], [5] with Green function:

$$i\tilde{n} \cdot D H_n(x - y) = i\delta^{(4)}(x - y) \quad (7)$$

- In Euclidean space, this becomes ($\tilde{n} = (in^0, \vec{n})$):

$$i\tilde{n} \cdot D_E H_{\tilde{n}}(x_E - y_E) = \delta^{(4)}(x_E - y_E) \quad (8)$$

- The tree level propagator suffers from tree-level UV cutoff effects in Euclidean space

Numerical implementation and strategy for extracting the CS kernel

Considerations for lattice computation:

- Cutoff effects from the auxiliary propagator [6], [7]
- Power divergence from finite length Wilson lines
- How to regulate ultraviolet divergences
- On the lattice r has an additive renormalization

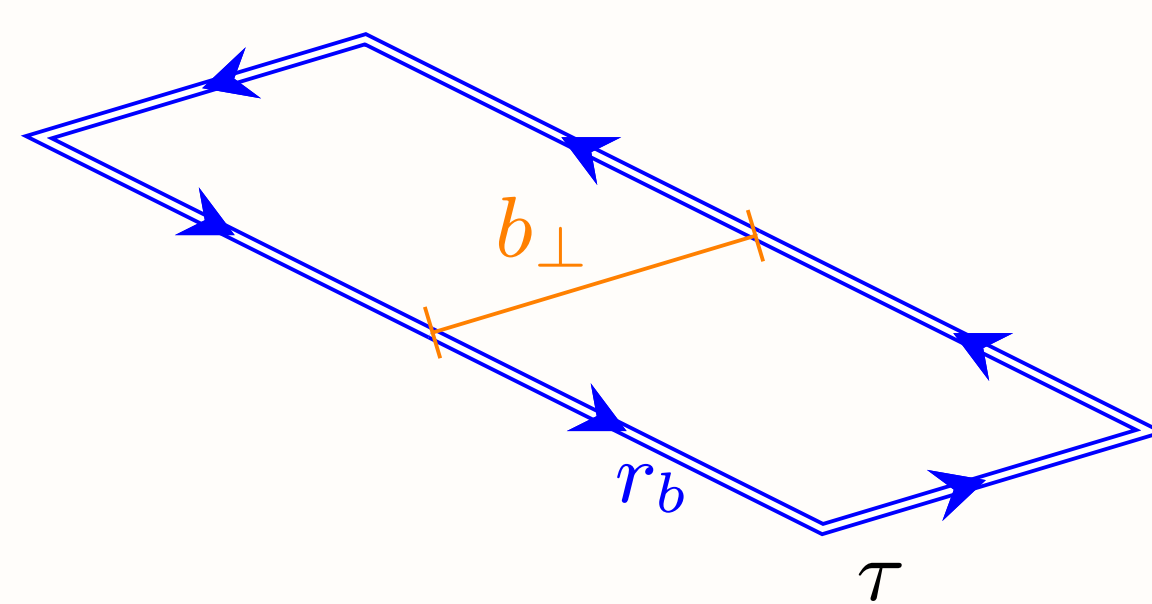


Figure 2: Schematic for rectangle loop, W_B . W_A can be drawn similarly.

"ratio method"

$$\frac{W_{\text{bfly}}(b_\perp, a, r_a, r_b)}{\sqrt{W_A(b_\perp, a, r_a, r_a) W_B(b_\perp, a, r_b, r_b)}} \quad (9)$$

- Gives the soft function *and* the CS kernel
- Removes cutoff effects and power divergences
- In practice, W_A and W_B on the lattice suffer from an extreme signal to noise problem
- Solving this is the subject of future work

"double ratio"

$$R_D \equiv \frac{W_{\text{bfly}}(b_\perp, a, r)}{W_{\text{bfly}}(b'_\perp, a, r)} \bigg/ \frac{W_{\text{bfly}}(b_\perp, a, r')}{W_{\text{bfly}}(b'_\perp, a, r')}, \quad (10)$$

where $r = r_a = r_b$ in each W_{bfly} .

- This method only gives the CS kernel
- ' b_\perp ' ratio removes cutoff effects
- ' r ' ratio removes power divergences

$$\log(R_D) = (\gamma_q(b_\perp, \mu)) - \gamma_q(b'_\perp, \mu) \times \log\left(\frac{r+1}{r-1} \bigg/ \frac{r'+1}{r'-1}\right) \quad (11)$$

Results

- Figure (3) demonstrates the cancellation of cutoff effects at large lattice time
- The double ratio removes the power divergence, as we don't see any linear dependence on b_\perp in Fig. (6)
- The small values in Fig. (6) suggest that the contributions to the r renormalization are large

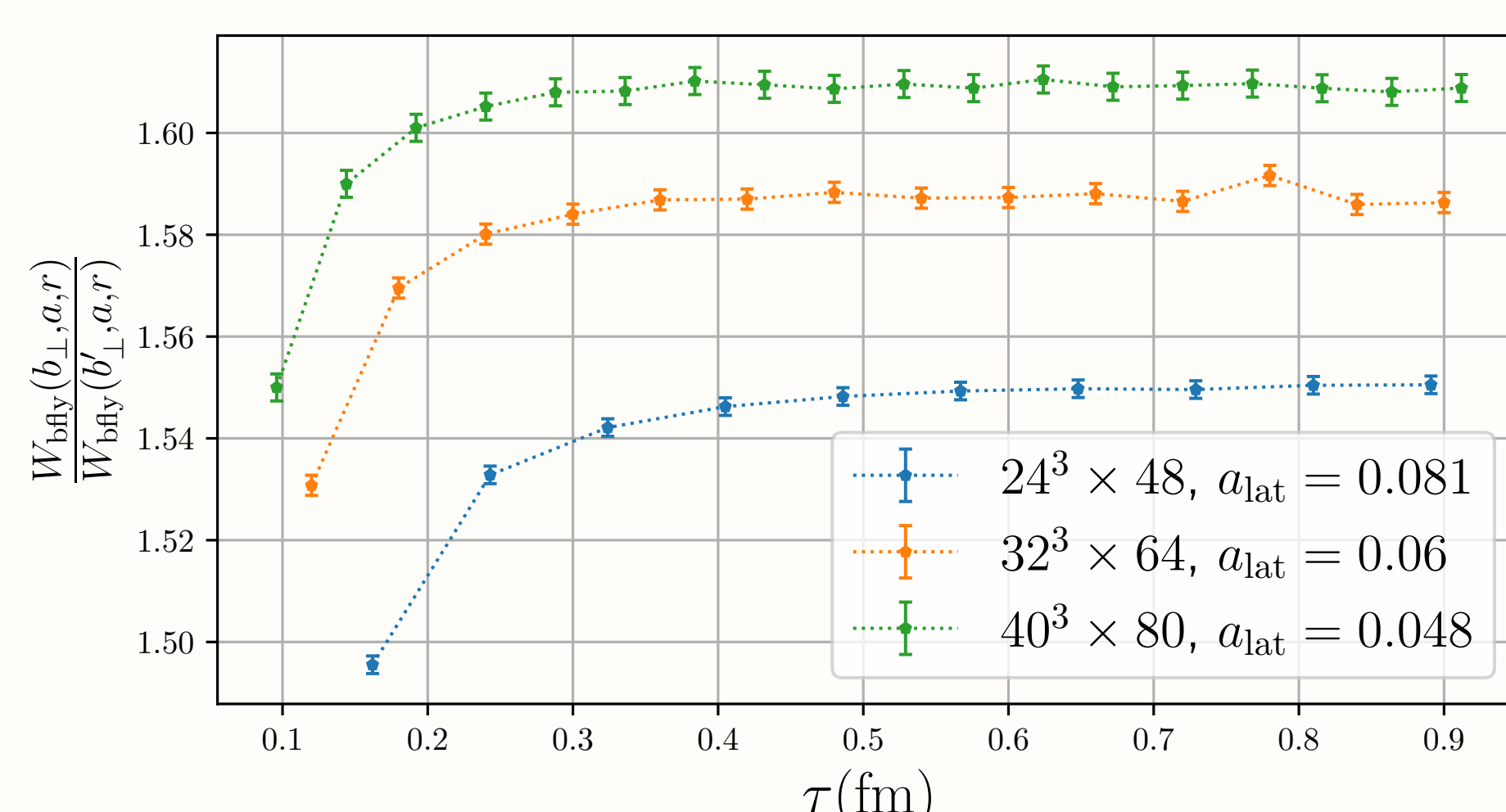


Figure 3: Time dependence of the ratio of butterfly loops at two different values of b_\perp . Here, we use $b_\perp = 5a$, $b'_\perp = 2a$, and $r = 1.001$.

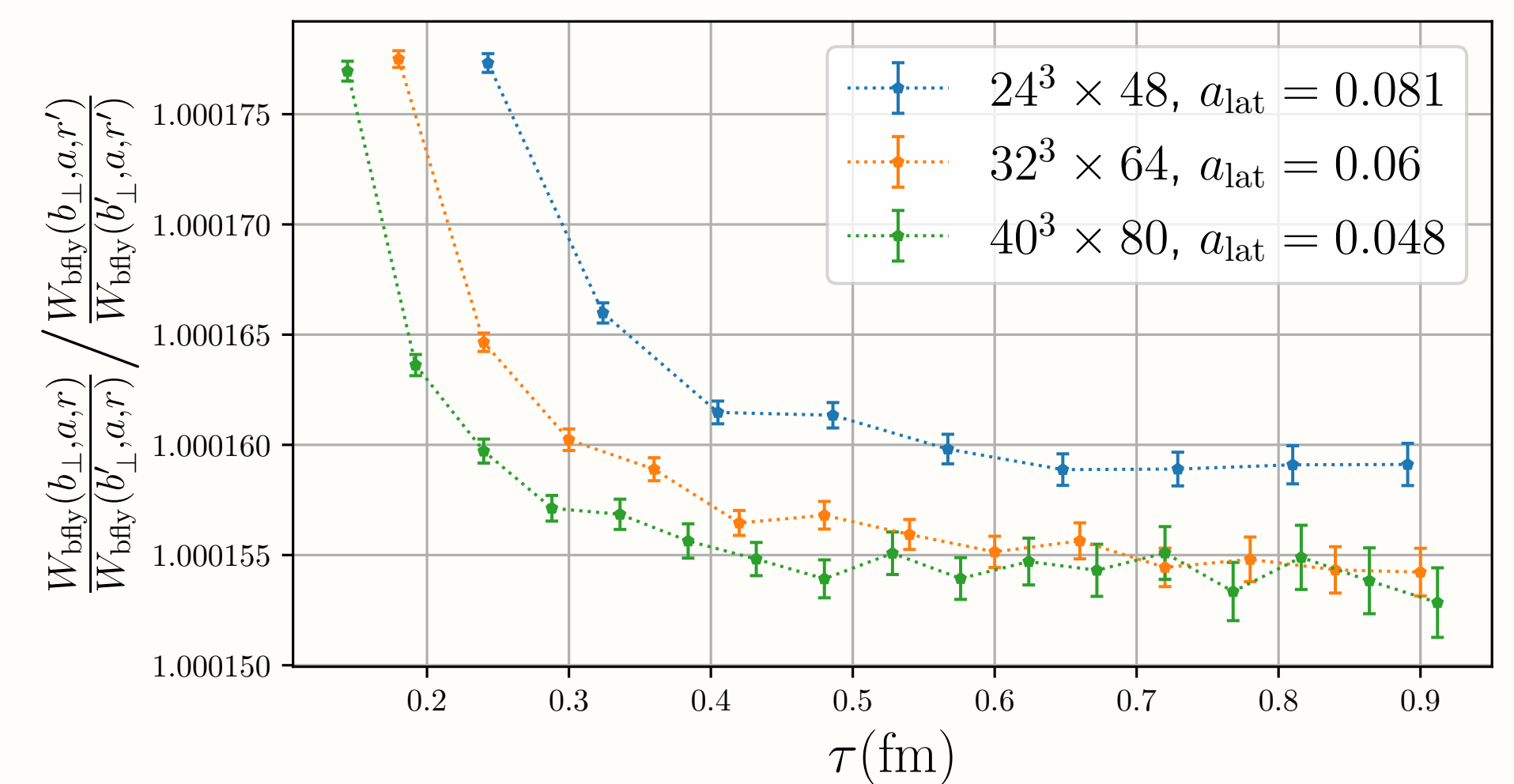


Figure 4: Time dependence of the double ratio. Here, we use $b_\perp = 5a$, $b'_\perp = 2a$, $r = 1.002$, and $r' = 1.001$.

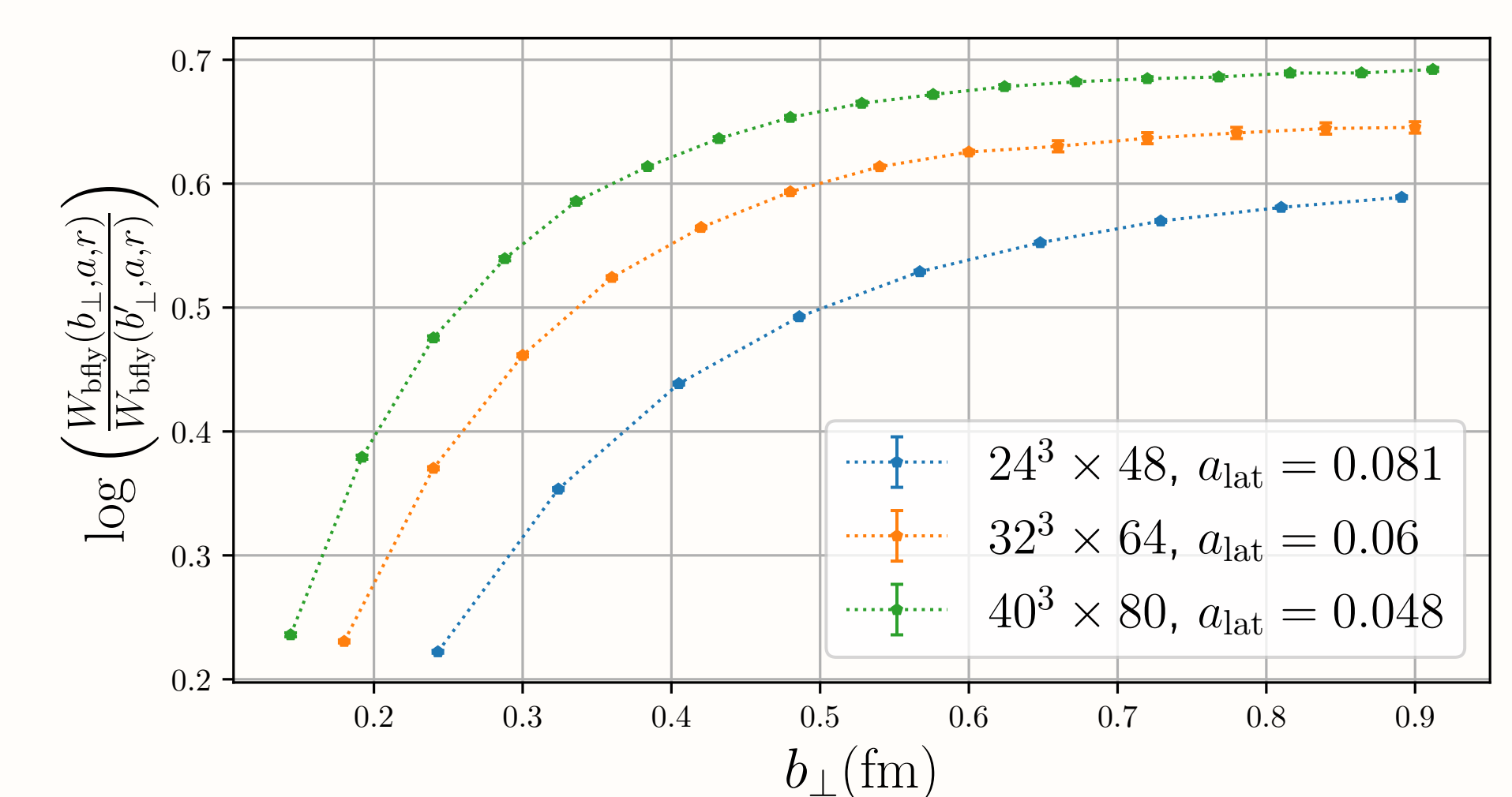


Figure 5: b_\perp dependence of the log of the single ratio. Here, we use $b'_\perp = 2a$, and $r' = 1.001$. We also take the largest possible τ on each lattice.

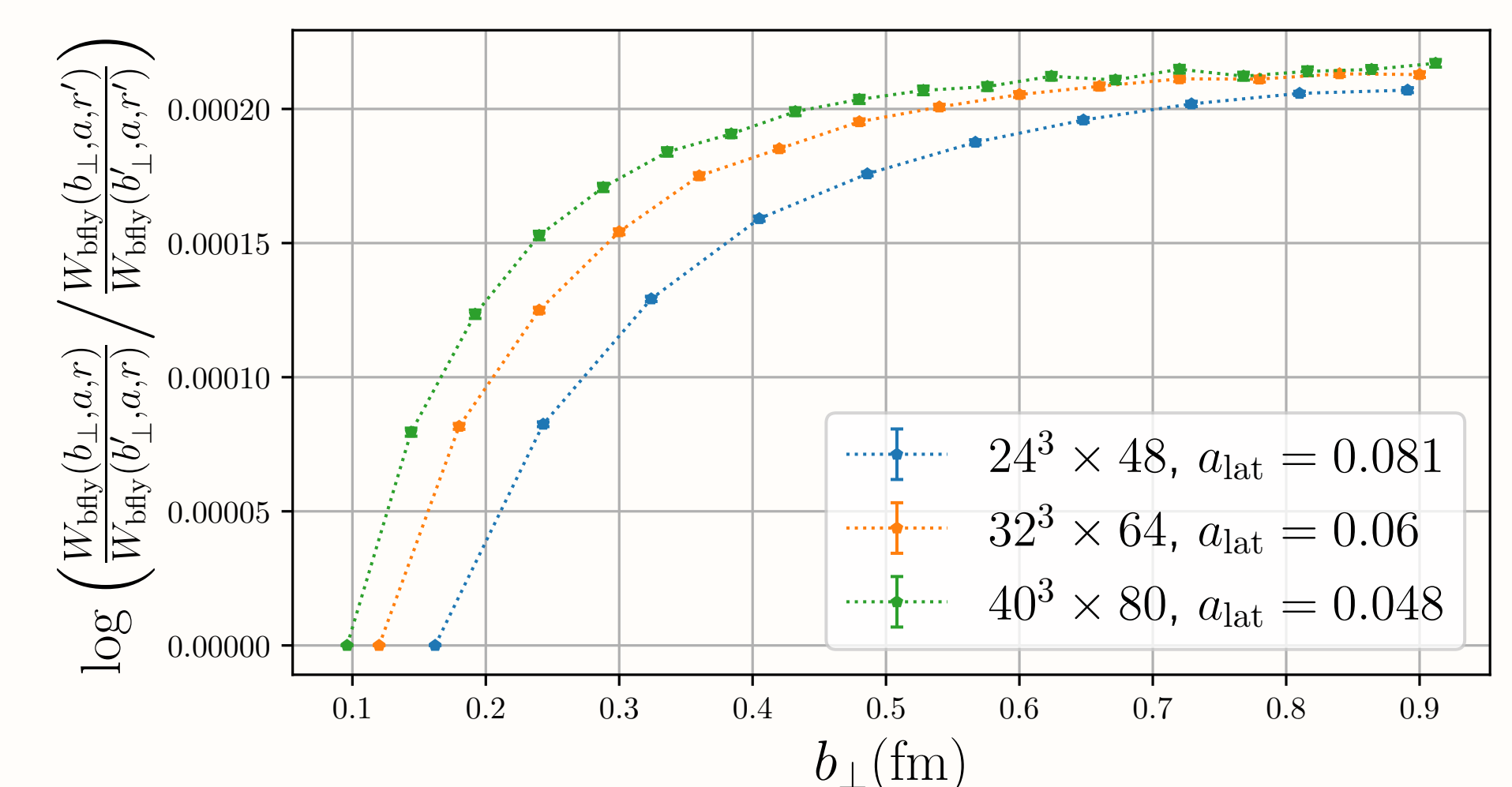


Figure 6: b_\perp dependence of the log of the double ratio. Here, we use $b'_\perp = 2a$, $r = 1.002$, and $r' = 1.001$. We also take the largest possible τ on each lattice.

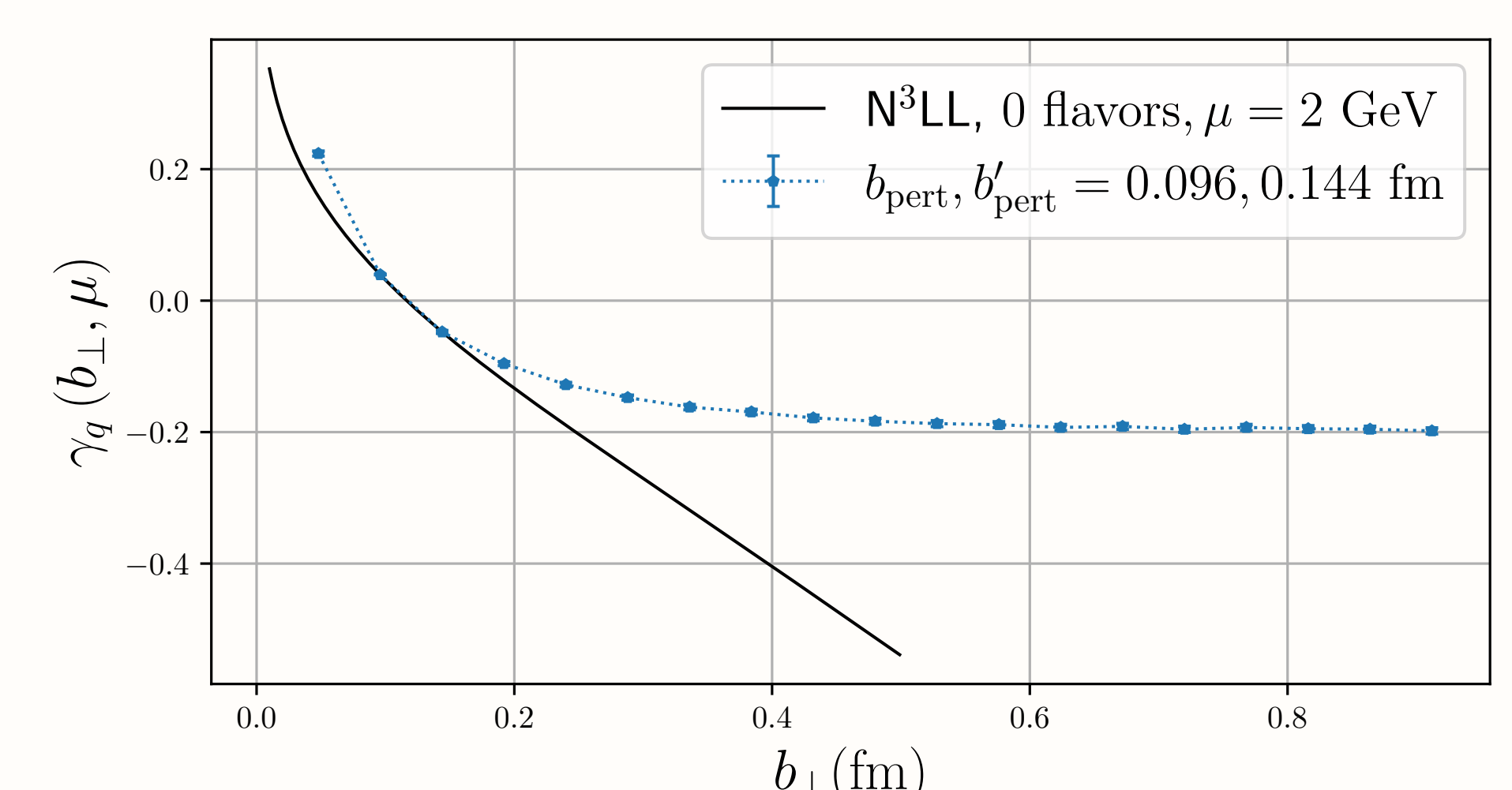


Figure 7: Preliminary extraction of the CS kernel, for the $40^3 \times 80$ lattice. We matched the lattice result in the perturbative region at $\mu_0 \sim 1/a$ and evolved to $\mu = 2$ GeV.

- We are working to quantify the contribution from the r renormalization
- We are able to obtain an incredibly high degree of statistical precision
- Still need to investigate the contributions from systematic error

[1] doi: 10.1016/j.nuclphysb.2020.115054. arXiv: 1910.11415 [hep-ph].

[2] doi: 10.1103/PhysRevD.99.034505. arXiv:1811.00026 [hep-ph].

[3] doi: 10.1017/9781009401845. [4] doi: 10.1016/0370-2693(80)90529-8. [5] doi: 10.1016/0550-3213(80)90397-1.

[6] doi: 10.1016/0370-2693(92)90695-Z. [7] doi: 10.1016/0550-3213(94)90231-3. arXiv: hep-ph/9304274.